MIT Libraries | DSpace@MIT

MIT Open Access Articles

Single element spectral splitting solar concentrator for multiple cells CPV system

Massachusetts Institute of Technology

Single element spectral splitting solar concentrator for multiple cells CPV system

Marco Stefancich,[1,2,*] Ahmed Zayan,[1] Matteo Chiesa,[1] Stefano Rampino,[2] Dario Roncati,[2] Lionel Kimerling,[3] and Jurgen Michel[3]

[1]*Laboratory For Energy and Nano Sciences, Masdar Institute of Science and Technology, Abu Dhabi, United Arab Emirates*
[2]*Istituto dei Materiali per l' Elettronica ed il Magnetismo, Consiglio Nazionale delle Ricerche, Parco Area delle Scienze 37/A - 43124 Parma, Italy*
[3]*Massachusetts Institute of Technology, 77 Massachusetts Avenue Cambridge, Massachusetts 02139-4307, Boston, USA*
[*]*mstefancich@masdar.ac.ae*

Abstract: Shockley Read Hall equation poses a limit to the maximum conversion efficiency of broadband solar radiation attainable by means of a single bandgap converter. A possible approach to overcome such a limit is to convert different parts of the broadband spectrum using different single junction converters. We consider here a different modus operandi where a single low-cost optimized plastic prismatic structure performs simultaneously the tasks of concentrating the solar light and, based on the dispersive behavior of the employed material, spatially splitting it into its spectral component. We discuss its approach, optical simulations, fabrication issues and preliminary experimental results demonstrating its feasibility for cost effective high efficiency Concentrated Photovoltaic Systems (CPV) systems.

OCIS codes: (230.1360) Beam splitters; (260.2160) Energy transfer; (040.5350) Photovoltaic.

References and links

1. W. Shockley and H. J. Queisser, "Detailed balance limit of efficiency of p-n junction solar cells," J. Appl. Phys. **32**(3), 510–519 (1961).
2. A. G. Imenes and D. R. Mills, "Spectral beam splitting technology for increased conversion efficiency in solar concentrating systems: A review," Sol. Energy Mater. Sol. Cells **84**(1-4), 19–69 (2004).
3. L. M. Fraas, J. E. Avery, J. Martin, V. S. Sundaram, G. Girard, V. T. Dinh, T. M. Davenport, J. W. Yerkes, and M. J. O'neil, "Over 35-percent efficient gaas/gasb tandem solar cells," IEEE Trans. Electron. Dev. **37**(2), 443–449 (1990).
4. W. Welford and R. Winston, *High collection nonimaging optics* (Academic Press, New York, 1989).
5. R. King, D. Law, K. Edmondson, C. Fetzer, G. Kinsey, H. Yoon, R. Sherif, and N. Karam, "40% efficient metamorphic gainp/gainas/ge multijunction solar cells," Appl. Phys. Lett. **90**(18), 183516 (2007).
6. E. D. Jackson, "Solar energy converter" (US Patent 2,949,498, 1960).
7. A. Barnett, D. Kirkpatrick, C. Honsberg, D. Moore, M. Wanlass, K. Emery, R. Schwartz, D. Carlson, S. Bowden, D. Aiken, A. Gray, S. Kurtz, L. Kazmerski, M. Steiner, J. Gray, T. Davenport, R. Buelow, L. Takacs, N. Shatz, J. Bortz, O. Jani, K. Goossen, F. Kiamilev, A. Doolittle, I. Ferguson, B. Unger, G. Schmidt, E. Christensen, and D. Salzman, "Very high efficiency solar cell modules," Prog. Photovolt. Res. Appl. **17**(1), 75–83 (2009).
8. J. D. McCambridge, M. A. Steiner, B. L. Unger, K. A. Emery, E. L. Christensen, M. W. Wanlass, A. L. Gray, L. Takacs, R. Buelow, T. A. Mccollum, J. W. Ashmead, G. R. Schmidt, A. W. Haas, J. R. Wilcox, J. Van Meter, J. L. Gray, D. T. Moore, A. M. Barnett, and R. J. Schwartz, "Compact spectrum splitting photovoltaic module with high efficiency," Prog. Photovolt. Res. Appl. **19**(3), 352–360 (2011).
9. B. Mitchell, G. Peharz, G. Siefer, M. Peters, T. Gandy, J. C. Goldschmidt, J. Benick, S. W. Glunz, A. W. Bett, and F. Dimroth, "Four-junction spectral beam-splitting photovoltaic receiver with high optical efficiency," Prog. Photovolt. Res. Appl. **19**(1), 61–72 (2011).
10. M. A. Green and A. Ho-Baillie, "Forty three per cent composite split-spectrum concentrator solar cell efficiency," Prog. Photovolt. Res. Appl. **18**(1), 42–47 (2010).
11. D. Vincenzi, A. Busato, M. Stefancich, and G. Martinelli, "Concentrating pv system based on spectral separation of solar radiation," Phys. Status Solidi A **206**(2), 375–378 (2009).

12. L. Fraas, J. Avery, H. Huang, L. Minkin, and E. Shifman, "Demonstration of a 33% efficient cassegrainian solar module," *in Proceedings of IEEE 4th World Conference on Photovoltaic Energy Conversion* (IEEE, 2006), pp. 679-682.

13. B. Groß, G. Peharz, G. Siefer, M. Peters, J. Goldschmidt, M. Steiner, W. Guter, V. Klinger, B. George, and F. Dimroth, "Highly efficient light splitting photovoltaic receiver," in Proceedings of 24th European Photovoltaic Solar Energy Conference (2009), pp. 130–134.

14. U. Ortabasi, A. Lewandowski, R. Mcconnell, D. J. Aiken, P. L. Sharps, and B. G. Bovard, "Dish/photovoltaic cavity converter (pvcc) system for ultimate solar-to-electricty conversion efficiency-general concept and first performance predictions," *in Proceedings of IEEE 29th Photovoltaic Specialists Conference* (IEEE, 2002), pp. 1616-1620.

15. R. Menon, "Ultra-high efficiency multi-junction solar cells using polychromatic diffractive concentrators" (US Patent 20100095999, 2010).

16. R. K. Kostuk and G. Rosenberg, "Analysis and design of holographic solar concentrators," *Proc*. SPIE **7043**, 1–8 (2008).

17. J. E. Ludman, "Holographic solar concentrator," Appl. Opt. **21**(17), 3057–3058 (1982).

18. J. M. Castro, D. Zhang, and R. Kostuk, "Planar holographic solar concentrators for low and medium ratio concentration system " *in Proceedings of Optics for Solar Energy* (Optical Society of America, Tucson, 2010).

19. C. Bainier, C. Hernandez, and D. Courjon, "Solar concentrating systems using holographic lenses," Sol. Wind Technol. **5**(4), 395–404 (1988).

20. W. H. Bloss, M. Griesinger, and E. R. Reinhardt, "Dispersive concentrating systems based on transmission phase holograms for solar applications," Appl. Opt. **21**(20), 3739–3742 (1982).

21. P. Sharlandjiev and B. Markova, "On fabrication of large format optoelectronic elements," J. Optoelectron. Adv. Mater. **5**, 39–44 (2003).

22. P. Borden, P. Gregory, O. Moore, H. Vander Plas, and L. James, "A 10-unit dichroic filter spectral splitter module," in Proceedings of IEEE 15th Photovoltaic Specialists Conference (IEEE, 1981), PP. 311-316.

23. J. Onffroy, D. Stoltzmann, R. Lin, and G. Knowles, "High-efficiency concentration/multi-solar-cell system for orbital power generation," in Proceedings of 15th Intersociety Energy Conversion Engineering Conference (1980), PP. 371-376.

24. D. Wagner and L. He, "An innovative solar system with high efficiency and low cost," *in Proceedings of IEEE 35th Photovoltaic Specialists Conference* (IEEE, 2010), pp. 003039-003042.

25. J. P. Penn, "High concentration spectrum splitting solar collector" (US Patent 6469241, 2002).

26. A. M. Fox, Optical properties of solids (Oxford Univ Press, 2010).

27. Schott Ag, "Abbe diagram for schott glasses," (2011), http://www.us.schott.com/advanced_optics/english/download/schott_abbe_nd_vd_pgf_july_2011_us.pdf.

28. J. D. Lytle, G. W. Wilkerson, and J. G. Jaramillo, "Wideband optical transmission properties of seven thermoplastics," Appl. Opt. **18**(11), 1842–1846 (1979).

29. F. Technologies, "Polycarbonate transmission coefficient," http://www.fresneltech.com/graphs/polycarbonate_graph.html.

30. J. Ward, K. Ramanathan, F. Hasoon, T. Coutts, J. Keane, T. Moriarty, and R. Noufi, "Cu (in, ga) se2 thin-film concentrator solar cells," *in Proceedings of NCPV Program review Meeting* (2001).

31. Y. Hirai, H. Nagashima, Y. Kurokawa, and A. Yamada, "Experimental and theoretical evaluation of cu (in, ga) se2 concentrator solar cells," Jpn. J. Appl. Phys. **51**(1), 04101 (2012).

32. A. Bechiri, F. Benmakhlouf, and N. Bouarissa, "Calculation of electronic and optical properties of zn-based ii-vi semiconductors," Phys. Procedia **2**(3), 803–812 (2009).

33. S. Chen, X. Gong, A. Walsh, and S. H. Wei, "Electronic structure and stability of quaternary chalcogenide semiconductors derived from cation cross-substitution of ii-vi and i-iii-vi_ {2} compounds," Phys. Rev. B **79**(16), 165211 (2009).

34. A. Luque, G. Sala, and J. Arboiro, "Electric and thermal model for non-uniformly illuminated concentration cells," Sol. Energy Mater. Sol. Cells **51**(3-4), 269–290 (1998).

35. P. G. Nelson, "An analysis of scattered light in reflecting and refracting primary objectives for coronagraphs" in *Technical Note 4* (Coronal Solar Magnetism Observatory, 2006).

36. D. W. Sweeney and G. E. Sommargren, "Harmonic diffractive lenses," Appl. Opt. **34**(14), 2469–2475 (1995).

37. M. T. Gale, "Replication techniques for diffractive optical elements," Microelectron. Eng. **34**(3-4), 321–339 (1997).

38. M. Mokhtar, M. T. Ali, S. Bräuniger, A. Afshari, S. Sgouridis, P. Armstrong, and M. Chiesa, "Systematic comprehensive techno-economic assessment of solar cooling technologies using location-specific climate data," Appl. Energy **87**(12), 3766–3778 (2010).

1. Introduction

Due to the spectral width of the solar emitted radiation, the efficiency of any single bandgap solid state converter is inherently limited on one side by the bandgap dictating the maximum wavelength capable of photogeneration and, on the other side, by the generation of "hot" carriers due to photons having energies much larger than the bandgap [1].

The simultaneous use of several junctions with different bandgap provides a firmer theoretical ground to achieve higher efficiencies with theoretical limits approaching 85% [2] through one of two methods: the first involves the use of stacked solar cells where cells with decreasing bandgaps are stacked on top of each other and connected in series. The bandgap decreases from the uppermost cell to the lowermost one [3] allowing the radiation that is not converted by the top cell to reach the lower one due to the material's transparency to radiation below its bandgap. The stacking imposes severe constraints on the materials and substrates choice due to lattice matching problems. Furthermore, the fabrication process of such cells, where the current trend uses on III-V materials, requires epitaxial growth processes on expensive substrates like GaAs and Ge. The approach is, therefore, commercially viable in terrestrial systems only under very high concentration to offset the high cell cost. This imposes strong requirements on the mechanical tracking systems to cope with the etandue limited angular acceptance [4] of high concentration systems. While MJ cells efficiencies have been for a few years in the region of 40%, the final efficiency of a commercially complete system under real operating conditions is in the region of 30% [5]. An alternative approach, proposed for the first time in the fifties [6], is to split the light into spatially separated spectral regions to be used with properly selected single junction solar cells. The main advantage of this approach is the accessibility to a broader group of cells since the stringent material and fabrication requirements for cell stacking no longer apply. Since the cells are physically separated, they can be even based on completely different, and cheaper with respect to epitaxial growth technologies. Moreover, the wider acceptance angle of the device allows for a higher optical efficiency, reduced system complexity and reduced demand on the mechanical tracking of the setup [4]. The validity of the approach is testified by the achievement of a module where laboratory efficiencies approaching 40% were reported in [7]. The design of a concentrating spectral splitting system is a formidably complex task where optics, cell characteristics and performances are deeply intertwined. In most cases, the separation of the concentrating optics and the spectral splitting component allows for a conceptual simplification as testified by some recent works where the spectral splitting system alone has been considered [8, 9]. Often when the full setup is considered, scientists rely on a combination of primary concentrator followed by a high quality dichroic mirror spectral splitting arrangement [2, 10, 11]. A dual focus Cassegrainian system employing a secondary dichroic element demonstrated 33% efficiency [12] under lab conditions. More recently different approaches have emerged like [13] where a light trapping assembly, two dichroic mirrors and 3 solar cells could achieve 34% efficiency. A cavity receiver where a cavity and multiple rugate filters promise ultimate efficiencies [14,15]. Diffraction based holographic optical elements (HOE) have been considered for spectral splitting due to their high dispersion [16, 17]. High diffraction efficiencies over wide wavelength windows are, however, inherently difficult to achieve [18] and while multiplexing technique can been employed to increase the useful spectral window [19, 20], coupling in the doubly exposed holograms limits the effectiveness of the device. Replication of dichromated gelatine (DCG) volume holograms, the most promising for wide spectral operating windows, requires the use of a master hologram and the scalability of this process to very large scales can be complex [21]. The use of separate components for concentration and spectral splitting results in some optical losses at every optical interface. In earlier works [22, 23], losses are assumed between 7 and 11% at each optical component. In [3], optical efficiency can be estimated from the published data to be in the order of 87%. A highly sophisticated optical system like the one suggested in [7] employing a state of the art anti-reflection coating (ARC) on all the optical components achieves 93% weighted efficiency. Higher number of optical components may also affect the overall system cost, assembly complexity and tolerance limits. Integrating the concentrating and spectral splitting actions in a single optical component that can be easily manufactured with well-established industrial technologies may offer a valuable contribution to the development of high efficiency and cost-effective photovoltaic conversion systems. Along this line we consider a

single optical element system, generalizing some already proposed successful solutions [15, 24, 25], that can be designed and realized in any optically dispersive material to simultaneously concentrate and split the solar light incoming from a specific direction. Unlike dichroic-based systems, where the splitting is in discrete wavelength groups, the design presented here provides a continuous "rainbow-like" splitting that can be adapted to different sets of single junction cells. This stems from the fact that the spectral splitting relies on the inherent optical dispersion of the employed material. We present the conceptual framework and the mathematical building model that can lead to different embodiments of the component. We view the aforementioned realizations as specific cases of a more general solution that can be optimized according to different merit functions. A discussion about the several possible optimization approaches and consequent trade-offs will follow and a possible design will be presented, simulated, realized and tested.

2. Optical design principles

The optical element is conceptually defined as a set of solid transparent prism each operating independently. Each prism is designed to deflect and split a polychromatic collimated light beam from a given direction onto the same area of a common receiving target. The resulting concentrated and spectrally divided beam is attained by the superposition of each prism contribution. The receiver target intercepts the beam exiting from the prism ensemble. Each of the prisms is oriented in such a way that the light rays of a specific reference wavelength are mapped on the same target area as in Fig. 1 or according to its intended purpose.
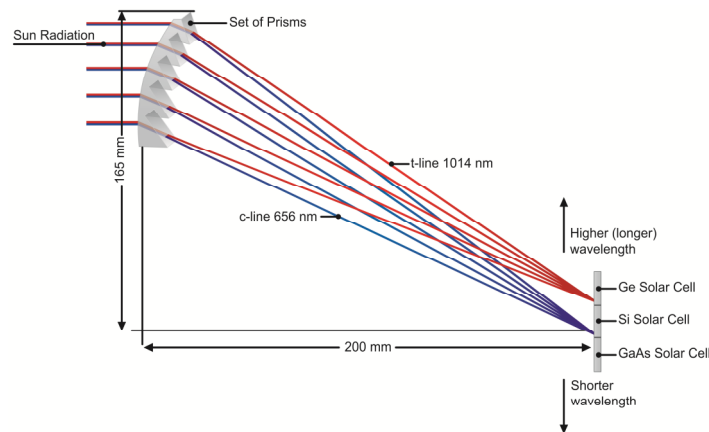

Fig. 1. Conceptual drawing of the concentrator/spectral splitting system with a detail of the beam splitting effect through part of the component. The system is a set of microprisms designed to deflect two reference wavelength on two distinct points on the photovoltaic receiver. The receiver does not need to be placed perpendicular to the optical axis and the proposed cells are just possible examples.

This prism-based approach provides a constructive design technique that can be adapted to different optical requirements and, in the limit of infinitely small prisms, provides a free form design tool. The design is two-dimensional and is extended in the third dimension by extruding the resulting 2-dim contour in the direction perpendicular to the page plane. This results in a linear 1-axis concentrator. The design can be extended, with a generalization of the mathematical derivation presented below, to a two-axis concentrator with a substantial increase of the attainable concentration. To better illustrate the constructive approach and the possible optimizations of the design we limit our consideration to the simpler 2D design to demonstrate the conceptual framework.

A prism made in a transparent dispersive material will split a collimated beam of light according to the wavelength due to the inherent dispersive characteristic of real materials

[26]. The basic element of the optical design is therefore a simple prism made in some dispersive material according to Fig. 2. Assuming collimated radiation, we define the optical "x" axis to be parallel to the direction of the light incident on the prism.
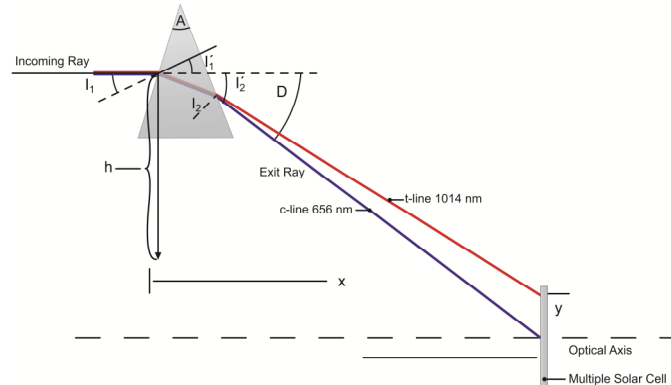

Fig. 2. The splitting by a single prism: A is the prism apex angle, I_1, I_2: Beam entrance/exit angle with respect to the relevant facets, r characterizes the rotation of the prism basis with respect to the optical axis (I_1 = A/2-r), h is the "height" of the entering light beam with respect to the reference center of the focal plane and x is the distance where the beam hitting the prism at height "h" encounters the focal plane where the cells are placed. D is the beam deflection angle between entrance and exit ray (wavelength dependent).

The essential parameters that affect the prism behavior are the angle formed by the entrance facet with the light rays (defined as I_1) and the apical angle of the prism (defined as A). Different choices of parameters would lead equivalent results through a different mathematical representation. With the above defined coordinates axis choice, the variable I_1 is the prism entrance facet inclination with respect to the vertical axis. The index of refraction is indicated with n_λ depending on the wavelength, in nanometers, of the considered light. The behavior of the n_λ depends on the choice of material, with materials having small Abbe coefficients being more prominent at efficient light splitting. Since the design of the primary collector in concentrator system is very sensitive to the raw material cost, the material choice must take into account industrial-feasibility, dispersion, transparency and cost effectiveness.

Different materials can be considered for the component with the two most important (optical) characteristics being a high chromatic dispersion coefficient (or equivalently a low Abbe number), and the average index of refraction and transparency over all the spectral region of interest (350 to 1500 nm). The high dispersion coefficient of many heavy flint glasses, like Schott N-SF66 with an Abbe number as low as 21, would make them suitable candidates but they are characterized by relatively high refractive indexes (>1.8). High values of the refraction index will induce higher reflection losses at the material/air interfaces and limit the geometry development due to a lower value of critical angle where total internal reflection will occur. On the other hand glasses with refractive index comparable with Polycarbonate (PC) (Abbe number 28, n=1.585) possess, in comparison, higher Abbe numbers [27]. Manufacturability and total cost of the component at the large-scale production is also an issue. While for plastics, it is possible to envision a large-scale injection molding approach where even small scale features can be reproduced reliably, a similar procedure for glass requires the development of more expensive equipment and is inherently more complex and energy intensive. Several commercial plastics could compete with PC but in some cases like PMMA, Zeonex and Ortorex dispersion is significantly lower while other like Polystyrene have lower durability. Commercial PC (Lexan) has also an optical transmittance, including Fresnel reflection losses, close to 90% for a 3.2 mm thick sample from 400 to 1100 nm and above 75% up to 1.6 microns [28, 29]. This combination of properties makes it a very interesting candidate for the development of the below described component. The

methodology can, however, be applied to any material once its dispersion characteristics are inserted in the model.

To model our device, we first studied the behavior of the single dispersive prism represented in Fig. 2. Based on the parameters I_1 and A, an analytical formula can be obtained providing the deviation angle between the incoming and exiting ray D_λ.

$$D_\lambda = I_1 - A + \sin^{-1}\left\{ n_\lambda \cdot \sin[A - \sin^{-1}(\frac{1}{n_\lambda} \cdot \sin(I_1))] \right\} \qquad (1)$$

A third degree of freedom is the angle formed between the surface of the photovoltaic multiple cells receiver (assuming it is flat) and the x axis. For the purpose of this demonstration, the receiver face was oriented perpendicularly to the optical axis. In specific merit functions where the maximization of the device's output is required, this angle can be altered. We finally label the distances "x" and "h" from the receiver center measured, along and perpendicularly to the optical axis respectively.

A reference wavelength is chosen and the parameters optimized such that the incident beam on the prism is deflected towards the center of the receiver.

This dictates the desired deviation "D" at the reference wavelength for the prism of interest as in Eq. (2) that can be inserted in Eq. (1).

$$D_{\lambda ref} = \tan^{-1}\left(\frac{h}{x} \right) \qquad (2)$$

We notice, however, that Eq. (1) has two free parameters (being I_1 and A). Therefore, it becomes vital to define a second condition to determine the prism geometry uniquely.

This is where the optimization process and choice of merit function enters into play. In some previously presented designs [15, 24], the entrance facet of each prism in the construction lays perpendicularly to the optical axis as in the classical configuration of a Fresnel lens. In this case, the deflection of the reference wavelength, together with the dispersion relation of the specific material, completely defines the behavior of the prism and the attainable beam splitting and optical system efficiency.

In this design, the entrance angle is not constrained, allowing for the optimization of the single prism design for the merit function described above. The final system is obtained by joining several optimized prisms to form a structure that closely resembles a double Fresnel lens operating both as concentrator and wavelength demultiplexer.

It is worthwhile discussing the definition of concentration level for this component because it involves both the optical concentration effect and the spectral spreading of the wide solar spectrum. For monochromatic radiation the concentration ratio is calculated taking into account that each prism will cast perfectly collimated light coming from the expected direction onto the same receiver area (this is actually true only at the two design wavelengths), having a transverse direction proportional to the prism (if the receiver is perpendicular to the original incoming beam). The optical concentration, therefore, grows with the number of prisms and with the inverse of the prism transverse dimension.

The solar beam divergence, however, increases the width of the concentrated line proportionally to the distance between concentrator and receiver. The effect can be quite substantial since long optical paths are necessary to spatially separate wavelengths in presence of small chromatic dispersions of the material.

For polychromatic beams, it must be noted that each spectral component is deflected on a different region of the collector, according to the element geometry and intrinsic dispersion curve of the material, with the deflection being non-linear as a function of the wavelength. A definition of the concentration ratio, therefore, depends on the considered wavelength window with the general rule that shorter wavelength are dispersed more than longer ones leading to lower concentration ratios in those regions. Spectral dispersion reduces the effect of geometrical concentration.

Referring to the specific example presented later in this work, the number of prisms, and therefore the monochromatic optical concentration at the design wavelength is 140X on a 1 mm wide line while the divergence corrected monochromatic concentration is 100X. For polychromatic beams the wavelength window between 730 and 1000 nm is deflected on a region having a width of 8 mm (including beam divergence effects) with an effective concentration of 17.5 . The shorter wavelength region from 400 to 730 nm is affected by a much larger change in refractive index of the material and is, therefore, spread out over a region 45 mm in width with an average concentration factor of 3.1. Simulated results for the wavelength between 1000 and 1500 nm provide a 16 mm wide collection region with concentration around 8.75.

3. Design optimization approaches and tradeoffs

As previously stated the optical setup can have up to 4 free design parameters: the two angles defining the prism, the angle formed by the receiver with the optical axis and the distance of the receiver from the vertex of the prism. While different parameter sets can be chosen, they are practically equivalent to those indicated. A fifth parameter could be the transverse dimension of the single prism but, smaller prisms will always provide better results ; hence the parameter is limited by the practical feasibility of the design and should be determined a priori.

It is worth noting that the system operates mapping a collimated beam of different wavelengths into beams characterized by exit angles that are a function of the wavelengths. The spatial separation of different wavelength on the receiver will therefore increase with increasing distance of the receiver from the optical element. For the same reason however, the system becomes more sensitive to angular tracking errors; causing a shift of the deflected beam that grows proportionally to the receiver distance may cause the "spillage" of some radiation outside the intended target. Similarly, the inherent divergence of the solar beam causes a blurring of a single wavelength line that is proportional to the receiver distance and will result in radiation spillage and wavelength overlap on the target.

In contrast, a shorter distance between concentrator and receiver allows for a more compact system but increases the angular divergence of the beam on the receiver, potentially increasing losses in radiation coupling unto the cells. Given the dimensions of the intended target cell where the reference wavelength must fall on, a possible choice for a preliminary, efficiency oriented merit function could be the power transfer efficiency from the prism to the cell. This takes into account, the radiation spillage effect due to beam divergence, tracking errors and the reflection losses at the cell's surface assuming a statistical angular distribution of the incoming radiation.

Since the optimization should refer to the whole concentrator, an iterative procedure is developed where the distance is chosen based on the prism located at the origin. Using that value, the simulation is performed, and later reconsidered to demonstrate its effect on the system.

The rotational angle of the receiver with respect to the optical axis will affect this merit function. This angle introduces an extra cosine factor in the optical concentration and skews the angular distribution of rays hitting the receiver. Aligning the receiver normal with the center of the concentrator provides the maximal flux and minimizes the angular distortion of the incoming rays' distribution.

Further degrees of freedom can be attained by relaxing the assumption that the cells are coplanar on the receiver. In this case, the optimization of this angle calls for an iterative procedure on the entire concentrator. In our experience however, the initial choice indicated above appeared to be the most viable and adding an extra variable to the already complex optimization procedure does not appear to be convenient.

The most relevant parameters for the optimization are those defining each single prism. The first point to note is that, according to Eq. (3), there is a relation between the beam deflection and the wavelength angular separation. After some manipulation, we get:

$$\frac{\partial D_\lambda}{\partial \lambda} = \frac{1}{n_\lambda} \cdot \frac{\partial n_\lambda}{d\lambda} \cdot \tan\left(D_\lambda - I_1 + A\right) \cdot \left(1 + \frac{\sin\left(I_1\right)}{\sin(D_\lambda - I_1 + A)} \sqrt{\frac{n_\lambda^2 - \sin^2(D_\lambda - I_1 + A)}{n_\lambda^2 - \sin^2(I_1)}}\right) \quad (3)$$

While the rightmost term is equal to 1 if the entrance facet is perpendicular to the incoming ray [15, 24], for most choices of parameters and materials, its values are between 0.5 and 2.

As from Eq. (1), D_λ is determined by I_1 and A, while the first part of Eq. (3) highlights the spectral splitting dependency on overall beam deflection and on the quantity $D_\lambda - I_1 + A$. It can be stated that, large angular separations between close wavelengths given the material specific dispersion curve, require high deflection of the beam from the prism. At the same time, optical losses due to reflection of the beam at the two interfaces with air, are dictated by Fresnel relations and tend to increase with the total beam deflection.

A key point to make note of is that different amount of reflection losses are associated to the same total beam deflection depending on the interplay between the I_1 and A. In general, the losses are higher if one of the two interfaces dominates the beam deflection, as it happens in the case where the angle I_1 is set to zero. If both surfaces contribute to the achievement of the desired beam deflection, a minimum in total reflection losses can be obtained.

In Fig. 3 several choices are made for the parameter I_1 of a polycarbonate prism where the parameter A is determined by the condition that a wavelength of 1000 nm must be deflected by 30 degrees. While the separation between this wavelength and a ray at 750 nm decreases with the increase of I_1 it is also apparent that a minimum in the Fresnel losses can be achieved with an optimal choice of the parameters.
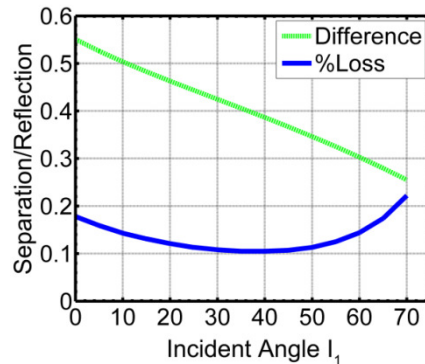

Fig. 3. Total reflection losses (blue) and angular separation (green, degrees) between two wavelength (750 and 1000 nm) for different configurations of a polycarbonate prism set to deflect the 1000 nm wavelength of 30 degrees.

Since the final objective is to transfer light to a defined set of physical cells, the angular wavelength separation is related to the desired physical separation between the wavelengths of interest, which by extension is related to the prism-receiver distance. Focusing on a single cell, we can define the lower and higher wavelength that we intend to concentrate on that area and proceed with the design and optimization. The preliminary merit function discussed above can therefore be extended to include the reflection losses caused by the prism where the dimension of the intended target cell and the wavelength window impinging on it are fixed parameters. The reflection losses and the radiation spillage are calculated for the extreme wavelength in the desired window and the optimization attempts, to maximize the total power transfer efficiency on the target cell by modifying the prism-receiver distance and the prism

angles. A more sophisticated approach would require the knowledge of the relative power density associated to the specified wavelength and the spectral response of the employed cell. In this case, a multi-wavelength optimization dependent on the cell and source could be carried out.

While the concentrator is completely determined by the conditions discussed above, the characteristics of the dispersed wavelength outside the reference wavelength window depend on the specific shape of the material dispersion curve. Once the system is optimized for the desired wavelength range, light with wavelengths longer than the lower cutoff will be deflected above the initial target cell while the shorter wavelength will be deflected below. In a 3-cell system, this allows placing a lower and a higher bandgap cell in these two positions respectively completing the spectral splitting system but does not leave any degree of freedom to tweak the characteristics of the power distribution outside the reference wavelength window. This is a consequence of employing a merit function that emphasizes only the element optical efficiency in a limited wavelength region. A different approach can be followed that takes into account what happens outside the central cell attempting to divert the radiation above and below the cutoffs onto cells of specific dimensions.

Once the specific merit function is defined, the use of Eq. (1) supported by the Fresnel limited calculation of the optical efficiency, for different wavelength allows us to fully define the prism parameters. In this discrete prism approach, once the position and parameters of the first prism are determined, the design of the complete concentrator follows with an iterative procedure where new prisms are added to the design and optimized, according to the specific algorithm. We will further demonstrate the afforested constructive procedure, with a specific set of requests for the optimization, to a specific system configuration.

4. Considerations about possible photovoltaic converters

Currently, the high efficiency photovoltaic conversion technological platform focuses on III/V because of the possibility to modulate the bandgap with different compositions combinations while preserving the lattice matching with GaAs or, preferably, Ge substrates (possibly Si-Ge virtual substrates). This is a key issue when multiple absorbers are stacked in Vertical Multi Junction cells. Moreover, while expensive and not easily scalable to large wafers, Ge is useful in the conversion of wavelength up to 1.6 microns.

The presented design aims to decouple, by spectral splitting, the cells used for different spectral region conversion providing a platform where no lattice matching constraints exists allowing for a larger set of spectrally matched converters to be considered. Short wavelengths can be converted by, as an example, Ga rich $Cu(In_xGa_{1-x})Se_2$, mid bandgap can be converted by either Silicon or, again, CIGS thin film cell [30, 31]. For long wavelengths, while much development is necessary, consideration could be given to $Hg_{1-y}Cd_yTe$ (y~0.6) or $Hg_{1-y}Zn_yTe$ (y~0.5) materials or even to more complex alloys [32, 33].

One of the key motivations for the reconsideration of spectral splitting approach is that it can spur the development for novel converter solutions by relaxing the lattice matching constraints of III-V.

It is worthwhile to consider, however, the issue of non-uniform illumination on the converters in this optical system. Non-uniformity in solar cell illumination can produce local temperature differences and contribute to ohmic losses because the cell operates locally at higher irradiance [34]. However the illumination non-uniformity associated with the continuous spectral splitting properties of this design, creating a rainbow like illumination pattern, is partially compensated by the line width thickening caused by the divergence of solar beam and by the finite size of each single prism. In addition, both thermal and ohmic loss effects are prevalent under high concentration conditions; this system is conceived to allow the use of multiple low cost technology cells under mid concentration levels (100 to 200X optical).

Another notable consequence of the spectral splitting approach is that, while Vertical Multi Junction (VMJ) are usually 2 terminal devices, the independent cells configuration in spectral splitting systems allow for greater degrees of freedom being a multi-terminal device.

In VMJ system the two terminal configurations requires current matching between the layers and this is achieved by adapting the layers thicknesses (affecting the absorption) and bandgap (and therefore the spectral response).

In spectral splitting systems, however, cells bandgap, dimensions and position in the split beam can be optimized independently for each generator, allowing the implementation of a similar current matching scheme. Cell position and dimension, in particular, affect the total amount of light collected by the cell and in turn, through the spectral response of the cell, the total amount of generated current.

Moreover, in a real spectral splitting system, the herein described element is replicated several times allowing to group in different ways multiple cells of the same typology.

Although a spectrally insensitive system MPPT optimization could be attained by series connecting each generator typology separately and feeding each channel independently to a multichannel inverter, this, may not be practical due to the multiplication of DC channels.

Conversely, a voltage matching scheme, unavailable to VMJ cells, can be also be devised. A proper number of cells of the same typology (larger number for lower voltage cells) can be connected is series between different optical elements to attain a MPPT target voltage common to all the channels. Voltage matched multiple channels can be then assembled in parallel with minimal disruption of each cell operation conditions. Since voltage is weakly dependent on illumination level, the configuration is stable both for intensity and spectral variation in the incoming radiation. As an example if the mid bandgap cell has an ideal MPPT of 0.55 V and the low bandgap cell has a 0.35 V, a 2 cells series connection for the mid bandgap and a 3 cells series for the low bandgap can be combined in parallel with minimal disruption of both MPPT. A 6 element optical system will provide 5 channels (2 with 3 low bandgap cells in series and 3 with 2 mid bandgap cells in series) that can be connected in parallel.

5. Component design

In our pilot design, we assume to employ 3 different cells for 3 wavelength windows comprised between 400, 730, 1000 and 1500 nm. We assume a linear dimension for the central cell of 8 mm. We moreover require that the concentrator theoretical optical efficiency does not fall below 85% on average, and that the total angular distribution incident on the receiver does not exceed ± 18 degrees.

The maximum receiver distance is determined a priori such that the single wavelength line spreading induced on the receiver by the solar divergence does not exceed 15% of the intended separation between the two central wavelengths and that a tracking error of ± 0.5 degrees does not shift the beam by more of 30% of the intended separation between these.

The single prism transverse dimension is set to 1 mm to induce a spreading smaller than 12% of the intended separation. The use of Eq. (1) for the central reference wavelength allows us to build the prism assembly by providing the values of I_1 and A for each prism once the vertex position is determined. The receiver distance is optimized by several tests to shape the distribution of the wavelength outside the mid-energy window on the two external cells.

While different choices of reference wavelength and building conditions could result in a more uniform wavelength spreading, we obtain that using a polycarbonate optical element, the wavelength from 1000 to 1350 nm are spread over a region of approximately 16 mm while the shorter wavelength from 400 to 730 nm are spread over a region of 45 mm. These dimensions and the cutoff wavelength are compatible with the use of low bandgap cells (e.g. Ge) and high bandgap cells (e.g. GaAs, CdSe) together with a Silicon mid bandgap cell.

6. Practical realization

While the theoretical design procedure discussed above is perfectly functional, to allow for the realization of the optical component, some modifications have to be applied.

To generate the prism assembly the first condition is set such that each prism in the structure is physically connected to an adjacent one. Each prism's top vertex is set to coincide with the leftmost bottom vertex of the prism immediately above it (Fig. 1 in the insert). This results in an assembly having a continuous entrance surface while the exit surface closely resembles that of a Fresnel lens.

However, for the mechanical stability of the assembly, it is necessary for the optical element to have a finite thickness everywhere. An extra thickness can be added to each prism translating the exit facet while maintaining parallelism with the initial one. A proper modulation of this extra thickness allows to render the design mechanically stable and to achieve a piecewise continuity of the exit facet of the optical device significantly reducing the number of sharp prism apexes typical in the Fresnel lens design.

The resulting geometry, generated by a suitable MATLAB code, is visible in Fig. 4 where the spectral separation effect on rays of two different wavelengths is demonstrated under the simplified assumption of perfectly collimated light.

The model was imported into a commercial raytracing tool and realistic optical simulations are performed to verify the predicted behavior.
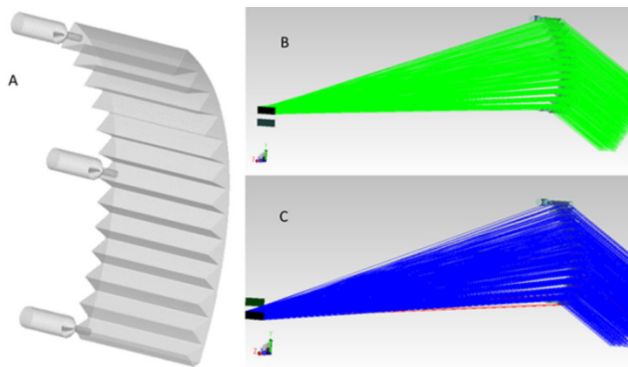

Fig. 4. The resulting concentrator design (A), the simulation of its behavior with perfectly collimated monochromatic light at two different wavelengths (B) and (C)

7. Raytracing based optical analysis

Two different optical analyses have been performed by means of a commercial raytracing package. The first assesses how effective is the device in directing the desired wavelengths on the designated areas if ideally sized receivers are used. The second one reproduces the actual experimental setup where a finite area light sensor is employed.

A controlled divergence beam impinging on the concentrator is defined according to the mathematical model. Figure 1 presents a pictorial representation of the raytrace configuration with light at two different wavelengths. The insert shows in detail the rays' behavior while crossing a part of the optical element. In Fig. 4, the two inserts present the actual results of the raytracing at two separate wavelengths demonstrating how the optical element manages to concentrate the two different reference wavelengths on two separate targets.

For the first ideal analysis the standard AM 1.5D spectrum was employed, in order to better reproduce the behavior of the optical device in experimental conditions, the second simulation was based on the solar spectrum reading acquired on site.

Different simulations are also performed introducing tracking inaccuracies up to ± 0.5 degrees and the result is simply an almost rigid displacement of the illuminated area on the receiver without significant modification in the spectral distribution. The choice of receiver-

concentrator distance allows us to maintain this effect in the expected and tolerable error range.

The effectiveness of the simulated concentrator in separating the different spectral component in the incoming light is demonstrated by dividing the receiver into 3 appropriately sized contiguous areas and analyzing the spectral distribution of the radiation on each area starting from the AM1.5D spectral energy distribution. The resulting configuration commands an area 45 mm long for the short wavelength collection region (SW, from 400 to 730 nm), 8 mm long for the mid wavelengths (MW, from 730 to 1000 nm) and 16 mm long for the longer wavelength (LW from 1000 to 1500 nm). The spectral distribution is summarized in Table 1.

Table 1. Spectral Distribution of Concentrated Radiation in Different Regions of the Receiver

	400-730	730-1000	1000-1350
SW	91%	9%	0%
MW	12%	76%	12%
LW	1%	28%	71%

Combining the power fluxes on all the three areas the overall optical efficiency of the system can be evaluated at 83.5% and is limited only by the reflection losses at the air/polycarbonate interfaces and the residual corners associated losses. Further improvements are possible by the use of proper ARC coatings, or by a different choice of optimization procedure.

The second performed simulation provides a comparison with the experimental results. Since the experimentally employed light collecting element has a finite dimension and does not entirely cover the receiver area, a different configuration of the simulated optical elements is employed. In this second case, the simulated radiation is collected by a circular element located to agree with that of the experimental one using the same shape and dimension.

The power collected by this element is then calculated, for each wavelength from 350 to 950 nm with a step of 10 nm. The long wavelengths cutoff is dictated by the experimental setup characteristics. The simulated results are collected in Fig. 5 for three different receivers position and clearly demonstrate the potentiality of the proposed optical device. The comparison with the experimental results is discussed in the following section.
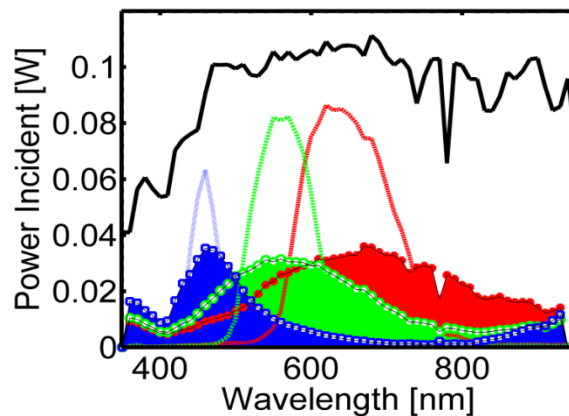

Fig. 5. Simulated (dashed lines) and experimental (full area curves) power distribution for 3 different positions of the integrating sphere.

8. Concentrator realization and experimental setup

The first attempt at the practical element realization was based on a subtractive technique performed on Computer Numerical Control (CNC) high precision machines. The advantage of this approach is that no investment cost was necessary and a very quick design-to-prototype time was possible. However, this approach cannot be generalized to larger scale production and resulted in poor quality of the realized element badly affecting the optical component performances. Despite its shortcomings, the element performed qualitatively as expected demonstrating the robustness of the design approach.

Since the tooling marks of the CNC process where several microns in size the optical component was post-processed by a fine polishing at low speed to avoid heat associated material degradation, to recover the components optical properties. This resulted in an RMS surface roughness of 40 nm, measured by AFM surface topology, where short wavelength components dominate. In the Gaussian approximation for surface roughness, this would induce- for a flat surfaces with quasi normal light incidence- a total integral scattering [35] of approximately 6% but since the component spectral separation relies on rays exiting from the prism close to the limiting optical angle, the scattering effect is significantly increased at the second PC/Air interface.

Lastly, the mechanical polishing process caused rounding of the prisms apexes significantly increasing Fresnel losses and inducing a spurious curvature radius to the supposedly flat prism surfaces.

Since, however, the mechanical polishing process will not be necessary if the part will be realized by injection molding, and the qualitative performance of the component has been demonstrated to agree with the design expectations, the inclusion of these effects in the optical model would not be of particular interest.

Injection molded components can achieve, with post processing chemical and thermal treatment, finishing of up to 25 nm RMS (and 15 nm with specialized optical processing [36, 37]) with reduction of total integral scattering for quasi normal incidence to less than 1%. Moreover, since no mechanical polishing is necessary, facets flatness and prism apexes are limited only by the mold quality and the fluid dynamical specifications of the material.

To test the concentrator in real condition it was chosen to operate under real solar illumination. This approach, while more complex compared to the use of a solar simulator, is advisable because the correct operation of the presented design relies on the limited divergence of solar light arriving on the concentrator and on a spectral match of the source with the sun. The effective beam separation is strongly affected by the optical divergence of the light source which in solar simulators is around an order of magnitude greater than the sun's ± 0.25 degrees divergence.

The concentrator and a movable integrating sphere are enclosed in a darkened box (with a properly designed entrance for sunlight) mounted on a biaxial sun tracker. The sphere, having an opening of 0.7 cm^2, is mounted on a movable stage in the region where the split beam is concentrated (Fig. 6) and the collected radiation is transferred by a multimode fiber to a spectrophotometer providing the necessary beam analysis.
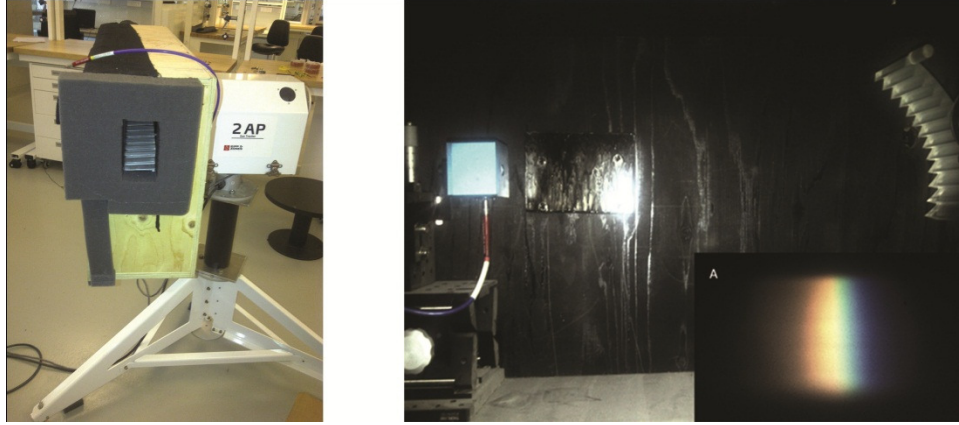
Fig. 6. An actual image of the outdoor data acquisition system. . The visible setup is actually assembled on a biaxial tracking system. An image of the actual split beam collected on a black diffuser is presented. The gradual transition between colors is visible.

The 980 nm cutoff of the silicon-based spectrophotometer prevents us from verifying the performance of the concentrator on the longer wavelengths region. If the model predictions are confirmed by experiment on the detectable wavelength region, we can, however, extend the results, taking into account the specific polycarbonate transmission curve, to evaluate low bandgap cells specific performances (e.g. Ge cells converting wavelength up to 1700 nm).

Due to the significant contribution of diffuse radiation at the experimental site [38] and residual scattering in the box, a background radiation removal procedure was applied.

In Fig. 5, we can see the spectral analysis of the normalized radiation collected in 3 positions on the concentration plane together with the total amount of radiation collected by the concentrator at each wavelength. In the same graph the simulated results are presented on the same scale. The comparison with the normalized experimentally collected, and undivided solar spectrum in Fig. 5, clearly shows how the optical device manipulates the spectral energy distribution.

While there is a qualitative agreement with the numerical simulations, the spectral distribution of the experimental data exhibits a much broader distribution in wavelength collected in each position and, a lower average intensity than that forecasted by raytracing. The latter is a direct result of the component's poor finish quality, whereas the former is a combination of both the component's quality and the site conditions.

Studies performed on the direct solar beam divergence detailed in [38] show that due to atmospheric dust levels and humidity, the apparent dimension of the solar disk at the experimental site (Abu Dhabi, UAE) is significantly larger than the conventionally assumed + −1/4 of degree. As implied from the previous theoretical analysis, this has detrimental effects on the sharpness of the spectral splitting obtained with the optical element. The off-axis radiation is deflected in slightly different positions on the receiver and overlaps with different wavelengths contained in rays that reached the component from the normal direction. This broadens the split spectrum impinging the receiver. Nevertheless, the robustness of the design is evident from the fact that, even with these negative factors, the attained spectral separation is suitable to demonstrate the effectiveness of the approach.

For a further quantitative estimate of the spectral division effect we divided the region between 430 and 950 nm into 2 arbitrary bands: long (between 950 and 730 nm), and short (between 400 and 730 nm) wavelength bands. We then compare based on the experimental data, the normalized energy distribution, in several different positions with the full spectrum (Fig. 7).
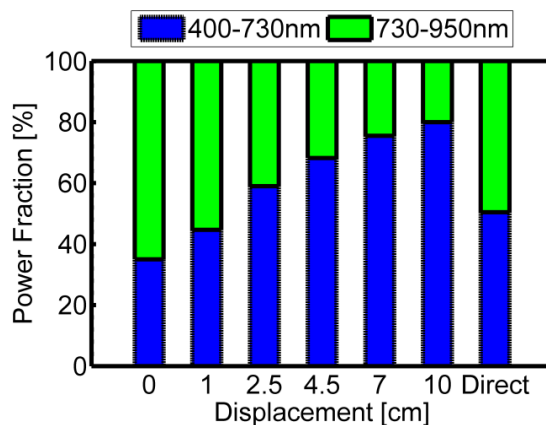
Fig. 7. Normalized power distribution across the receiver. The different areas in the graph correspond to the amount of energy arriving on each receiver between 400 and 730 nm (blue region), and between 730 and 950 (red).

9. Conclusions

We attempt a generalization and theoretical analysis of a promising approach for single component spectral splitting and concentration of sunlight [15, 24] for the simultaneous use of different solar cells removing the constraints of vertical multi junction solar cells.

A constructive and general merit function based design approach is detailed for the optical element that can be adapted to different converters combinations and specifications. A specific realization is proposed, optimized, simulated, realized and experimentally tested.

The concept of attaining concentration by linear superposition of simple prisms is a powerful tool for a constructive approach to the design of non-imaging concentrator optical components.

The results obtained are in general agreement with the simulations demonstrating the robustness of the design despite it being a subject to unfavorable conditions.

While further development of the design and realization technique is necessary, we believe that, together with the former results, this demonstrates the feasibility of the approach for a cost effective single element spectral splitting concentrator.